JOURNAL OF GEOPHYSICAL RESEARCH, VOL. 116, F01004, doi:10.1029/2009JF001473, 2011

Computer simulations of self-organized megaripples in the nearshore

E. L. Gallagher[1]

Received 28 August 2009; revised 27 September 2010; accepted 12 October 2010; published 29 January 2011.

[1] Megaripples are bed forms with heights of 20–50 cm and lengths of 1–10 m that are common in the surf zone of natural beaches. They affect sediment transport, flow energy dissipation, and larger-scale hydro- and morphodynamics. They are thought to be dynamically similar to bed forms in deserts, rivers, and deeper marine environments. Here a self-organization model (similar to models for subaerial bed forms) is used to simulate the formation and development of megaripples in the surf zone. Sediment flux is determined from combined wave and current flows using stream power and bed shear stress formulations as well as a third formulation for transport based on simple rules, which represent sheet flow. Random bed irregularities, either imposed or resulting from small variations in transport representing turbulence, are necessary seeds for bed form development. Feedback between the bed and the flow, in the form of a shadow zone downstream of a bed form and increasing flow acceleration with elevation over the crests of bed forms, alter the transport such that organized bed forms emerge. Modeled bed form morphology (including cross-sectional shape and plan view) and dynamics (including growth and migration) are similar to natural megaripples. The model can be used to extend the field observations of Clarke and Werner (2004), which suggest that, if conditions remain the same, megaripples will continue to grow. Contrary to many bed form models, this model supports the idea that bed form spacing grows continually.

Citation: Gallagher, E. L. (2011), Computer simulations of self-organized megaripples in the nearshore, *J. Geophys. Res.*, *116*, F01004, doi:10.1029/2009JF001473.

1. Introduction

1.1. Megaripples in the Nearshore

[2] Megaripples are bed forms with heights of up to 50 cm and lengths of 1–10 m that occur frequently in the nearshore [*Clifton et al.*, 1971; *Clarke and Werner*, 2004, CW04 from here on]. They can be long-crested, but are often short-crested (~2 m) and irregular in shape (oval or lunate). *Gallagher* [2003] hypothesized that they are similar to dunes in rivers [*Nittrouer et al.*, 2008; *Jerolmack and Mohrig*, 2005] and deserts [*Werner*, 1995], as well as sandbanks, sand waves, and megaripples in tidal inlets and on the continental shelf [*Sterlini et al.*, 2009; *Idier et al.*, 2004, and references therein; *Dyer and Huntley*, 1999; *Ernstsen et al.*, 2005]. However, megaripples in the nearshore are altered by the combined wave and current flows of the surf zone [*Gallagher*, 2003]. They are most common in the shallow surf zone (<2 m water depth) but are also observed as patches in deeper water (2–5 m water depth) [*Gallagher et al.*, 2003]. Like bed forms in other environments, megaripples affect sand transport through increased suspension by turbulence in their lee, as well as through bulk transport via migration [*Gallagher et al.*, 1998; *Ngusaru and Hay*, 2004]. They act as hydraulic roughness elements, changing wave energy dissipation and water circulation patterns [*Garcez-Faria et al.*, 1998]. In addition, they are thought to be the source of hummocky cross stratification in sedimentary sequences and therefore are used to interpret ancient environments [*Duke et al.*, 1991]. However, they are not accounted for in models for sediment transport, morphodynamics, wave transformation, or nearshore circulation. A model to predict megaripple occurrence and dynamics likely would improve all components of nearshore modeling and the interpretation of the sedimentary record.

[3] To predict bed forms in oscillatory flow, *Clifton* [1976] developed an empirical model where bed forms increase in size from small orbital ripples to cross-ripples to megaripples with increasing stress until the bed is planed-off during sheet flow conditions. Regime-type models like *Clifton*'s [1976] are a common way to describe bed forms and have been developed for many different environments [e.g., *Raudkivi*, 1990] and lead to empirical predictors where bed form length and height are a quantitative function of the flow [*Wiberg and Harris*, 1994; *Nielsen*, 1981]. These models assume that for a given flow field there is a single equilibrium bed state. *Gallagher et al.* [2005] and *Hay and Mudge* [2005] found evidence for the occurrence of megaripples, smaller ripples, and flat beds under similar conditions, contrary to the regime-type model where different bed

[1]Department of Biology, Franklin and Marshall College, Lancaster, Pennsylvania, USA.

0148-0227/11/2009JF001473

form types exist independently and only for specific conditions. This contradiction to the regime-type and empirical models is also seen in other environments and for other features [*Middleton and Southard*, 1984; *Austin et al.*, 2007].

[4] Instability type models (both linear and nonlinear) find the wavelengths and dynamics of unstable bed modes in coupled fluid dynamic and bed evolution models [*Hulscher*, 1996; *Sterlini et al.*, 2009; *Idier et al.*, 2004; *Blondeaux*, 2001]. These models can predict realistic wavelengths for bed forms in many different environments, including ripples, sand waves, sand banks, and offshore megaripples. *Idier et al.* [2004] observed different types of bed forms occurring at the same time. To create different bed form length scales, they manipulated the bed roughness in the model (including sand grain roughness, bed form roughness, and boundary roughness owing to waves). However, usually only one wavelength is predicted in instability models and these features begin at full length and grow in amplitude.

[5] From unprecedented observations of bed forms using a video camera mounted on a high cliff overlooking the surf zone, CW04 observed megaripples forming and growing over multiple tidal cycles and they found that megaripples began as small features and their lengths grew continuously (growth was linear for younger bed forms <~0.5 days old and logarithmic for bed forms older than ~0.5 days). This is in contrast to equilibrium bed predictors (regime-type and empirical models) and instability model predictions, which both predict a single wavelength for certain conditions and not continuous wavelength growth. From their observations, CW04 hypothesized that megaripples will always occur inside the surf zone. Only changes in flow that occur too quickly for bed form adjustment or water depth changes such that bed forms enter the swash or approach the breakpoint will destroy the bed forms.

1.2. Self-Organization

[6] It has been suggested that many different types of morphological patterns are self-organized, including river meanders [*Stolum*, 1996], river dunes [*Jerolmack and Mohrig*, 2005], sorted-patterned ground [*Kessler and Werner*, 2003], sorted bed forms (e.g., ripple scour depressions on the continental shelf) [*Coco and Murray*, 2007], beach cusps [*Coco et al.*, 2000], wind ripples [*Nishimori and Ouchi*, 1993], and aeolian dunes [*Werner*, 1995]. In each of these complex systems, patterns emerge from nonlinear interactions between the system and the environment, from dissipative processes such as friction, turbulence, and sediment transport, and from being open (both material and energy are exchanged across system boundaries) [*Werner*, 1999].

[7] *Werner* [1995] used a "hierarchical" approach [*Ahl and Allen*, 1996] to model self-organized systems, where processes at different temporal and spatial scales are distinct from each other and can be separated. For example, the physics of sediment transport on the scale of the sand grains (e.g., hierarchical level 1) is a system that is difficult to model, because of the large number of sand grains and their interactions. To then simulate the motions of enough grains to predict a large-scale morphological feature like a dune (level 2) would be extremely expensive computationally. Trying to simulate height and length statistics, or spatial distribution of dunes in a dune field or migration rates (level 3) based on level 1 physics is currently impossible. *Werner*'s [1995] hierarchical model included transport of sediment slabs by wind (level 1) using only a few simple rules that sensibly represented the motion of sand being forced by a fluid, thus neglecting the complex, nonlinear physics at the individual grain scale. Instead the model emphasized the interaction between the bed form and the gross movement of air and sand (level 2). This interaction or feedback was the important self-organizing force that drove the emergent characteristics of the bed forms. *Jerolmack and Mohrig* [2005] developed a similar model for river dunes that used physics-based expression for sediment transport, but, like *Werner* [1995], incorporated the feedback between the bed and the flow explicitly and created realistic bed features. Interestingly, *Jerolmack amd Mohrig* [2005] found that turbulence or noise in the forcing flow field was imperative for creating morphologically and dynamically realistic features.

[8] Here a hierarchical, self-organization model for nearshore bed forms is developed and tested. Predicted features are compared with observations of bed forms in the natural surf zone. Transport is calculated in three different ways, verifying that the physics at the grain scale can be abstracted and used to drive bed form scale processes. As with previous modeling efforts, feedback is shown to be necessary for building and maintaining bed forms. Also, like *Jerolmack and Mohrig* [2005], flow turbulence (or a random variation in the flow) is shown to be important for initial bed form creation and realistic growth. The present model produces megaripples that are similar to those observed in the nature, including features observed in steady flow, purely oscillatory flow, flow with superimposed steady currents and naturally irregular measured flows from the nearshore. The growth of the bed forms predicted by the present model is shown to qualitatively reproduce the observations of CW04, both of which behave as predicted by the model by *Werner and Kocurek* [1999] with early wavelength growth that is fast and slows as the number of "defects" (bed form terminations) decreases.

2. Model

[9] The present model is similar to *Werner*'s [1995] model and is used to predict megaripple occurrence and morphology. The model consists of a matrix of stationary sediment slabs that is 256 × 256 in the horizontal and begins as 100 slabs deep (effectively infinitely deep). Each slab represents a 10 cm × 10 cm × 1 cm deep block of sediment. This first matrix represents a spatial domain or a region of a stationary bed. A second matrix (256 × 256) represents sediment that is in motion. The sand slabs are picked up from the first matrix (the stationary bed matrix) and placed in the second matrix (the moving matrix) (1) using simple rules (outlined below) and (2) with two widely used sediment transport formulations from the literature [*Bailard*, 1981; *Ribberink*, 1998]. Sediment transport is driven by the water velocity u above the bed, which is represented by a third matrix layer. The fluid layer is a single layer with no depth dependence and can be thought of as a free stream velocity as is commonly used to drive transport models. Water velocity is modeled (1) as a sinusoid plus a codirectional steady current and (2) with measured velocities from a natural surf zone. For each time step (1 s), the flow is the same at all

locations in the flow matrix except for an imposed random spatial fluctuation (*va*) intended to represent local turbulence (except in the test with no fluctuation). Clearly, this does not represent true, full-spectrum turbulence, because it has only a single time scale of 1 s and a single spatial scale of 10 cm^2 in the horizontal, but it serves to provide a randomly varying component, which is necessary for bed form creation and for creation of realistic bed forms [*Jerolmack and Mohrig*, 2005].

[10] The mean bed slope over the whole domain is zero and the local slope of the bed is not allowed to exceed 17° (lower than the angle of repose but accurate for the highly dynamic bed in the nearshore) by moving a block to a neighboring block, if the height of the starting location is more than three blocks higher than the neighbor. This is done in the stream-wise and then the cross-stream directions, thus allowing transverse (cross-stream) motion of sediment. This step is repeated until all slopes are below the threshold. There is a periodic boundary, so material leaving one end of the domain returns at the opposite end.

[11] *Werner*'s [1995] rules for sediment transport represented aeolian saltating sediments. Here the simple rules governing sand motion represent subaqueous transport of sand in the nearshore. In the natural surf zone, during peak flows (e.g., under a wave crest) a thick layer of sediment at the bed moves like a carpet (sheet flow). As the water slows down and reverses direction, much of the sand is put down. Then, on the return flow of the wave, sediment is transported again as sheet flow in the opposite direction. In the model, when u is larger than a threshold value, sediment slabs are picked up or mobilized and when u drops below the threshold value, the sediment is put down or redeposited on the bed. The thresholds used here to pick up or put down sand were chosen using the transport equation from *Bailard* [1981] for guidance (equation (1), Table 1, W = 1.5 cm/s). For example, if u = 70 cm/s, the calculated volume transport Q is about 0.75 cm^3/s and at u = 85 cm/s, Q is about 1.5 cm^3/s. These values of volume transport were roughly translated as the number of blocks that the given flow could pick up. With that, any flow between 70 and 85 cm/s was considered capable of picking up one block of sand. Below 70 cm/s, Q is less than 0.75 cm^3/s and the flow is not considered strong enough to support blocks anymore, so sediment blocks that are up in the moving matrix are put back into the stationary bed matrix. Using these coarse calculations, the threshold values were chosen from calculated values of transport (Table 1) to represent reasonable transitions, especially with this model that has distinct layers. The thresholds used for the present calculations are

if $|u_{ij}| \leq 50$ cm/s, put all sand down from position *i,j* in the moving matrix,

if $50 < |u_{ij}| \leq 70$ cm/s, put down half the sand from position *i,j* in the moving matrix,

if $70 < |u_{ij}| \leq 85$ cm/s, pick up 1 block from position *i,j* in the bed matrix,

if $85 < |u_{ij}| \leq 100$cm/s, pick up 2 blocks from position *i,j* in the bed matrix,

and if $|u_{ij}| > 100$cm/s, pick up 3 blocks from position *i,j* in the bed matrix,

where the subscripts i and j represent the location in the matrix. Using these rules, model slabs are lifted from the stationary bed matrix (for u > 70 cm/s) and placed into a moving matrix and are then available to be moved (more below). For u < 70 cm/s, slabs are taken from the moving matrix and placed back in to the bed matrix.

[12] Sediment is also picked up using two physics-based sediment transport formulations from the literature. According to *Bagnold* [1966], the transport of sediment in steady flows is proportional to the stream power. *Bailard* [1981] adapted that model for unsteady flows in the nearshore, with transport, Q, given by

$$Q = \frac{\rho_w C_f \varepsilon_b}{(\rho_s - \rho_w) g \tan\varphi}\left[|u|^2 u - \frac{\tan\beta}{\tan\varphi}|u|^3\right] + \frac{\rho_w C_f \varepsilon_s}{(\rho_s - \rho_w) g W} \cdot \left[|u|^3 u - \frac{(\varepsilon_s \tan\beta)}{W}|u|^5\right], \tag{1}$$

where u is the free stream velocity, $\tan\beta$ is the slope of the bed (the local slope is calculated from the bed matrix), $\tan\phi$ is the angle of repose of the sediments (0.3 is used for 17°), W is the fall velocity of the sediment (1.5 cm/s is used), ρ_w and ρ_s are the densities of the water and sediments (1 and 2.65 gm/cm^3 are used), g is gravitational acceleration, C_f is the coefficient of friction (0.003 is used here), and ε_b and ε_s are efficiency factors. Following *Bailard* [1981], ε_b = 0.135 and ε_s = 0.015 are used here (see Table 2).

[13] In the second transport formulation used here [*Ribberink*, 1998], transport is related to the bed shear stress via the Shields parameter [*Meyer-Peter and Mueller*, 1948]. Transport Q is given by

$$Q = 11\sqrt{\frac{\rho_s - \rho_w}{\rho_w} g D_{50}^3}\,(|\theta| - \theta_c)^{1.65}(\theta/|\theta|), \tag{2}$$

with the Shields' parameter θ given by

$$\theta = \frac{0.5 f_w (\rho_s - \rho_w)}{g D_{50} \rho_w}|u|u, \tag{3}$$

and $\theta_c = \theta$ using 25 cm/s as a threshold velocity. D_{50} is the mean grain size (0.2 mm is used here), g is gravity, and f_w is the wave friction factor (0.01). With both of the physics-based transport models, although Q is the volume transport, it is used directly to give the number of slabs picked up (1 cm^3/s results in 1 block picked up and calculated values of transport are rounded to whole numbers).

[14] Once sand slabs have been picked up, they are moved with the flow a distance that is proportional to the flow magnitude, which is given by

$$jump_{ij} = u_{ij} * jf * \mathrm{d}t, \tag{4}$$

where $jump_{ij}$ = 1 indicates a move from one matrix location (i,j) to the immediate neighbor $(i + 1,j)$, jf is the fraction of the velocity that a block jumps (with units of jumps/cm), and dt is the time step (dt = 1 s is used for all the present simulations). Because each block is 10 × 10 cm, jf = 0.1 gives transport at the same rate as the water itself, i.e., if u = 100 cm/s, then a block will jump 10 units or 100 cm in one time step. This is the upper limit for jf, because if jf is larger, sediment will move farther than the water particles, which is physically unrealistic. For the examples shown here, jf = 0.05 is used and represents the transport of a block of sand approximately half the distance of a water particle

Table 1. Values of Transport Q Calculated Using the *Bailard* [1981] Transport Formulation (Equation (1)) Driven by the Given Water Velocities u[a]

u (cm/s)	50	60	70	80	85	90	100	110	120	140	160
Q (cm^3/s) with W = 1.5 cm/s	0.2	0.4	0.75	1.2	1.5	1.9	2.8	3.9	5.5		
Q (cm^3/s) with W = 3 cm/s	0.15	0.3	0.5	0.8	1.0	1.2	1.7	2.4	3.3	5.7	
Q (cm^3/s) with W = 9 cm/s	0.1	0.2	0.35	0.5	0.65	0.8	1.1	1.5	2.0	3.3	5.3

[a]These values were used to choose the thresholds in the simple rules transport formulation.

in one time step. This was chosen to crudely represent the fact that boundary layer velocity (where the sediments are moving) is generally smaller than free stream velocity (the prescribed flow field). During each time step, slabs are picked up (or put down) according to the transport model used (simple rules, Bailard or Ribberink), added to (or removed from) the moving matrix, then each cell of the moving matrix is moved according to its local value of $jump_{ij}$. If slabs are not put down in one time step, they remain in the moving matrix and are put down or moved during subsequent time steps.

[15] An important aspect of the self-organization model is feedback between the flow and the bed, included here by adjusting the flow over a bed form. Two feedback mechanisms are used in the present simulations: (1) a shadow zone in the lee of a bed form, implemented by changing u over a downstream slope that is 17° (three blocks high) to $u/100$ (effectively 0) and (2) a velocity increase over higher bed forms to simulate flow acceleration over the crest of a bed form. In the present simulations, a velocity increase that is directly proportional to the height of the bed above mean bed level is used, e.g., a bed elevation that is 5 cm above mean bed level will experience a 5 cm/s velocity increase. This crude model for acceleration is based on intuition only. Future iterations of the model could employ more complex boundary layer flow formulations. No acceleration or deceleration is applied at bed elevations below the mean bed level. These two mechanisms are implemented at every cell in the matrix, thus altering the velocity matrix for further iterations.

[16] These two feedbacks were chosen because they represent commonly observed alterations to the flow field owing to bed forms [e.g., *Fredsoe and Deigaard*, 1992; *Middleton and Southard*, 1984; *Jerolmack and Mohrig*, 2005, and many others]. For example, when bed forms become steep, they experience flow separation over their crests such that flow immediately downstream of the crest is altered. Sometimes flow separation results in complex circulation and turbulence in the lee of a bed form. Here this flow separation is implemented simply with a reduction in the flow velocity to effectively 0 cm/s, representing a shadow zone only (Figure 1a). The second feedback mechanism represents flow constriction and acceleration that happens over the crest of a tall bed form. Flow constriction is particularly important in shallower water depths, where the bed form height may be a significant fraction of the overall water depth. In the surf zone, where water depths are usually less than 2 m, this depth constraint and resulting flow acceleration are implemented with the second feedback mechanism (Figure 1b).

[17] The effect that each of these mechanisms has on bed form development is illustrated in Figure (1). Erosion and accretion occur because of divergence or convergence of sediment transport. The shadow zone in the lee of a bed form (Figure 1a) causes a convergence of transport at the crest of the bed form resulting in accretion. At the base of the slope, a divergence of transport occurs, which leads to erosion. Therefore the shadow zone feedback acts to build bed forms with accretion at the crest and erosion in the trough. The acceleration of water up the stoss (or upstream) slope of the bed form, results in an increase in transport with elevation and a sediment divergence giving erosion (Figure 1b). Thus, this feedback mechanism acts to restrict the amplitude of the bed forms and slow their growth.

3. Results

3.1. Formation and Characteristics

[18] The results of this preliminary model (Figure 2) show a striking resemblance to observed megaripples [*Hay and Wilson*, 1994; *Gallagher et al.*, 2003, CW04]. For example, the predicted bed forms have wavelengths of 2–5 m and amplitudes of a few tens of centimeters, and they are generally short-crested with a crescentic shape if there is a steady flow and irregular and oval-shaped if the flow is purely oscillatory: in plan view they look similar to observed megaripples. The modeled bed forms do become taller than natural bed forms and they grow faster. These discrepancies will be discussed further later. Bed configuration predicted by the model using the simple rules and *Ribberink* [1998] formulations are shown in Figures 2a and 2b, respectively. Results using the *Bailard* [1981] sediment transport formulation (not shown) are similar to Figure 2b. Although

Table 2. Parameters in the Transport Formulae, the Values Used in the Present Study, and Common Ranges for Those Parameters

Parameter	Value Used	Common Range
W (fall velocity)	1.5 cm/s	1–9 cm/s
D (grain size)	0.2 mm	0.1–0.6 mm
tan β (bed slope)	Average slope = 0, local slope is calculated and constrained to < 17°	–
tan ϕ (angle of repose)	0.3 (17°)	0.1–0.8 (~10°–40°)
ρ_w, ρ_s, g	1.0 g/cm^3, 2.65 g/cm^3, 980 cm^2/s	constants
C_f (coefficient of friction)	0.003 [*Church and Thornton*, 1993]	0.0006–0.012 [*Garcez-Faria et al.*, 1998]
ε_b (bed load efficiency factor) [*Bagnold*, 1966]	0.135 [*Thornton et al.*, 1996], 0.13 [*Bailard*, 1981]	0.11–0.14 [*Bagnold*, 1966]
ε_s (suspended load efficiency factor) [*Bagnold*, 1966]	0.015 [*Thornton et al.*, 1996], 0.01 [*Bailard*, 1981]	0.01 [*Bagnold*, 1966]
f_w (wave friction factor)	0.01 [following *Ribberink*, 1998]	0.005–0.04 [*Fredsoe and Deigaard*, 1992]
jf (jump fraction)	0.05	0.1–0.01 (see text)

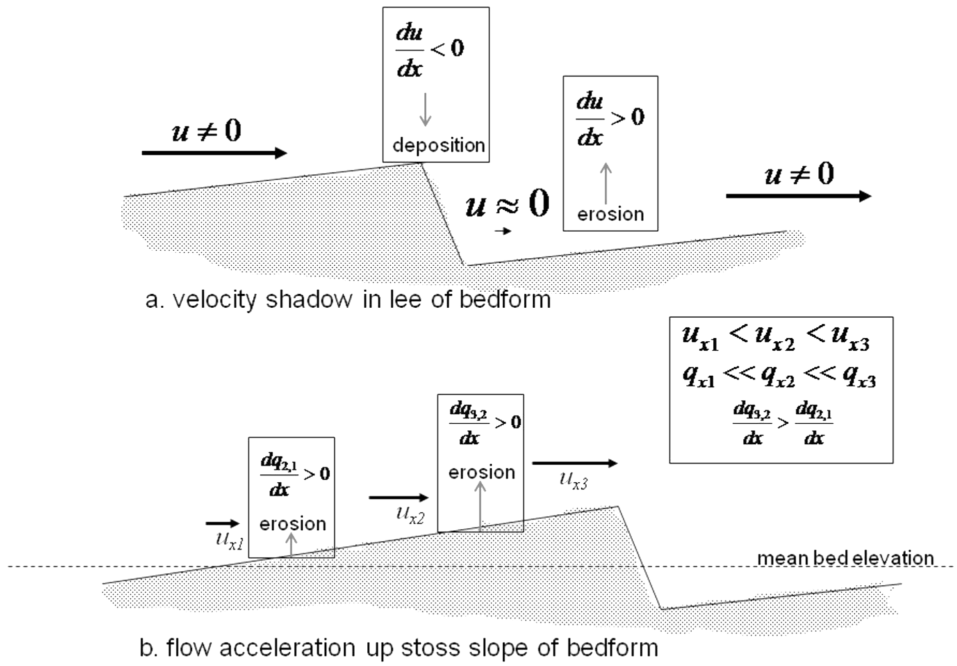

Figure 1. Illustration of feedback mechanisms employed by the model. (a) There is a velocity shadow in the lee of the bed form owing to flow separation such that the velocity becomes very small when there is a steep downstream-facing slope. Figure 1a illustrates that u is large, both upstream and downstream of the slope, but near the slope (within two block lengths), the velocity is approximately zero (velocity is divided by 100). The gradient in velocity and therefore in transport (q) will cause erosion and deposition. (b) As a bed form becomes larger, it will constrict the flow above it, causing the flow to accelerate as it flows up the stoss (or upstream) slope of the bed form. Figure 1b illustrates that, as the flow accelerates, there is a gradient in sediment transport q.

the amplitudes of bed forms from different simulations (Figures 2a and 2b) are slightly different, both types of transport models produce similarly shaped features.

[19] Using the model to examine megaripple formation processes, it is found that bed forms will never form from a flat bed without a perturbation. The turbulent component (*va*) provides spatial variability in the flow and variations in sediment transport across the domain. These variations lead to an initial perturbation on the bed surface upon which a feedback mechanism can work. Random perturbations of the bed surface (with *va* = 0) have the same effect (Figure 2c) and have been observed in nature [*Hay and Speller*, 2005]. Note that in Figure 2c, *va* = 0 for the whole simulation, resulting in bed forms that have distinct crests on a flat bed surface. This is compared with the smoothed, less distinct features predicted with a spatial flow variation (turbulence). The effect of *va* on model results is discussed further in Appendix A.

[20] As has been observed in many morphodynamic processes, the growth of bed forms is owing to feedback between initially small perturbations on the bed and the flow. Once feedback is established, orderly bed forms emerge and grow, and the feedback is reinforced. This concept is tested and verified here by removing the feedback mechanisms. In Figure 2d, with conditions identical to Figure 2a, the velocity shadow feedback mechanism (Figure 1a) is disabled. Irregularities form on the bed owing to random variations in the transport, but no bed forms grow from those perturbations. If the acceleration-with-elevation feedback mechanism (Figure 1b) is disabled, bed forms will grow quickly and become excessively tall and steep (Figure 2e). Thus, the first mechanism acts to build bed forms and the second mechanism acts to control amplitude growth.

3.2. Growth

[21] The model predicts that bed forms begin as irregular lumps and, via feedback between the flow and the bed form, evolve into short-crested bed forms and then into longer-crested, longer wavelength bed forms (Figure 3). As bed forms continue to evolve, smaller, faster bed forms merge with larger, slower ones, causing crest and wavelengths to grow. This merging and lengthening is observed in nature (e.g., CW04) and in other modeling studies [e.g., *Coco and Murray*, 2007; *Werner and Kocurek*, 1999; *Jerolmack and Mohrig*, 2005]. In Figure 2, the bed forms are all relatively young, having only grown for 13 min (~800 s) and most have short, irregular crests. In Figure 2e, the second feedback mechanism, which slows amplitude growth, was removed, so these bed forms grew faster and have developed longer crests in the same model time period. In Figure 3, a time series of predicted bed forms is shown, and these were allowed to grow for a longer time (1500 s) than the examples in Figure 2. Over this longer time period, the lengthening of both wavelength and crest length is observed.

3.3. Shape

[22] Because bed forms with lower amplitudes propagate more rapidly, small lumps catch and merge with larger

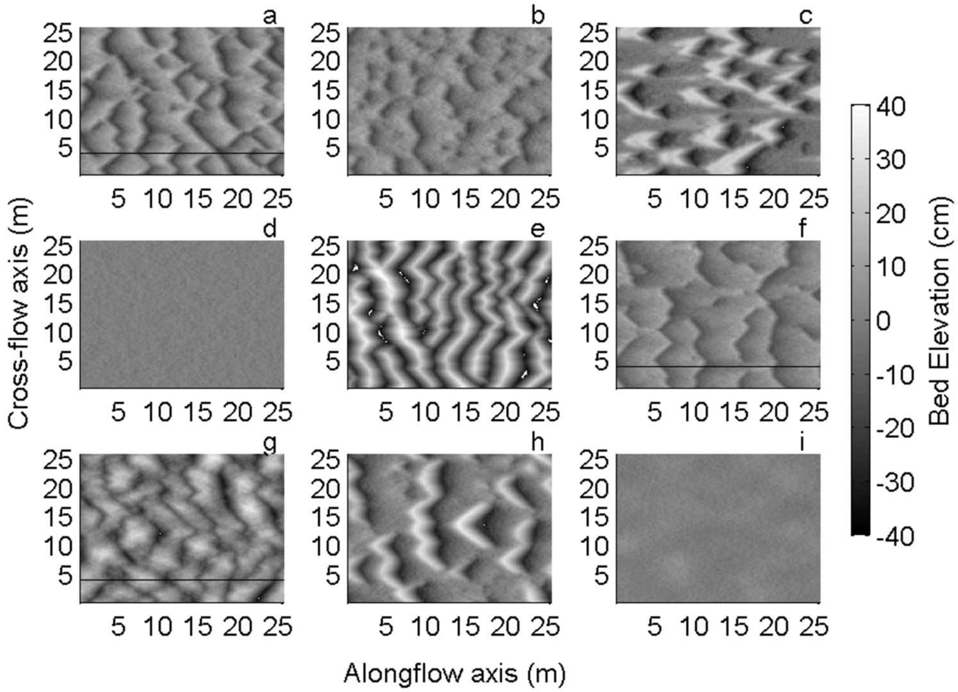

Figure 2. Plan view of simulated bed forms starting from a flat bed (except where noted). In Figures 2a, 2b, 2c, 2d, and 2e, A = 75 cm/s, T = 10 s, S = 20 cm/s (to the right), va = 15cm/s, and the simulation was run for 13 min (or ~800 s). In Figures 2a, 2c, 2d, and 2e, the simple rules transport formulation was used. In Figure 2b, the transport model from *Ribberink* [1998] was used. In Figure 2c, the conditions are the same as in Figure 2a, except va = 0, and the initial perturbation was from a spatially random 2 cm variation of the bed height. In Figures 2d and 2e, conditions are the same as in Figure 2a, but in Figure 2d, the shadow zone feedback mechanism was disabled and in Figure 2e, the acceleration-with-elevation feedback mechanism is removed. In Figure 2f, a steady flow only (A = 0 cm/s, S = 50 cm/s, va = 15 cm/s) is used to drive the model with the simple transport rules for 13 min. In Figure 2g, the steady flow was removed: A = 95 cm/s, T = 10 s, S = 0 cm/s, va = 15 cm/s, and the simulation (with the simple rules transport formulation) was run for 13 min. In Figure 2h, measured velocities from the natural surf zone were used and the simulation, with the *Ribberink* [1998] transport formulation, was run for 4.2 h. In Figure 2i, the model was run for an additional 13 min, starting from the bed in Figure 2a, but the feedback mechanisms were both removed. Lines in Figures 2a, 2f, and 2g are the locations of the profiles shown in Figure 4.

lumps contributing to the growth of bed forms with time. Similarly, the flanks of irregular bumps move forward faster than the larger crests, resulting in lunate or crescentic features, if there is a net transport in one direction (Figures 2a, 2b, and 2c). A net transport in one direction also results in features that have an asymmetric profile, with a steep lee (or downstream) slope and a shallowly sloped upstream face. Using steady flow only (Figure 2f), the present model predicts highly asymmetric (Figure 4a), three-dimensional (lunate, barchan or barchanoid ridge) features that migrate downstream and are similar to those observed and predicted in aeolian flows [*Bagnold*, 1941; *Werner*, 1995] and in rivers [*Jerolmack and Mohrig*, 2005]. In the nearshore, there are often combined flows (waves plus steady flows), resulting in net transport in one direction with a superimposed oscillatory flow. These nearshore flows generate bed forms that are lunate [Figure 2a, 2b, 2c; *Ngusaru and Hay*, 2004] and asymmetric (Figure 4b), but whose asymmetry is reduced by the oscillatory wave motions. In dominantly oscillatory flows in nature, where net flows are very small, the bed forms lose their lunate shape and their directionality, and they become oval-shaped features that are symmetric in profile [*Gallagher*, 2003]. These oscillatory flow-dominated features are well-predicted by the model (Figures 2g and 4c).

4. Discussion

[23] The results presented above validate the hierarchical approach and confirm that the details at the smallest scale can be abstracted in different ways with little effect on the modeled processes at larger scales. This is illustrated specifically in Figures 2a and 2b, where two different transport models are employed, each based on different physics (*Ribberink* [1998] based on shear stress and simple rules from *Bailard* [1981], which is based on energy expenditure or stream power) and yet the model consistently produces similar features. This concept is also supported by the shapes of predicted bed forms (in plan view and in profile), which are similar to features observed in different flow environments (e.g., rivers, outside the surf zone, within the surf). The one predicted parameter that does change significantly is the rate of growth of the bed forms. If tran-

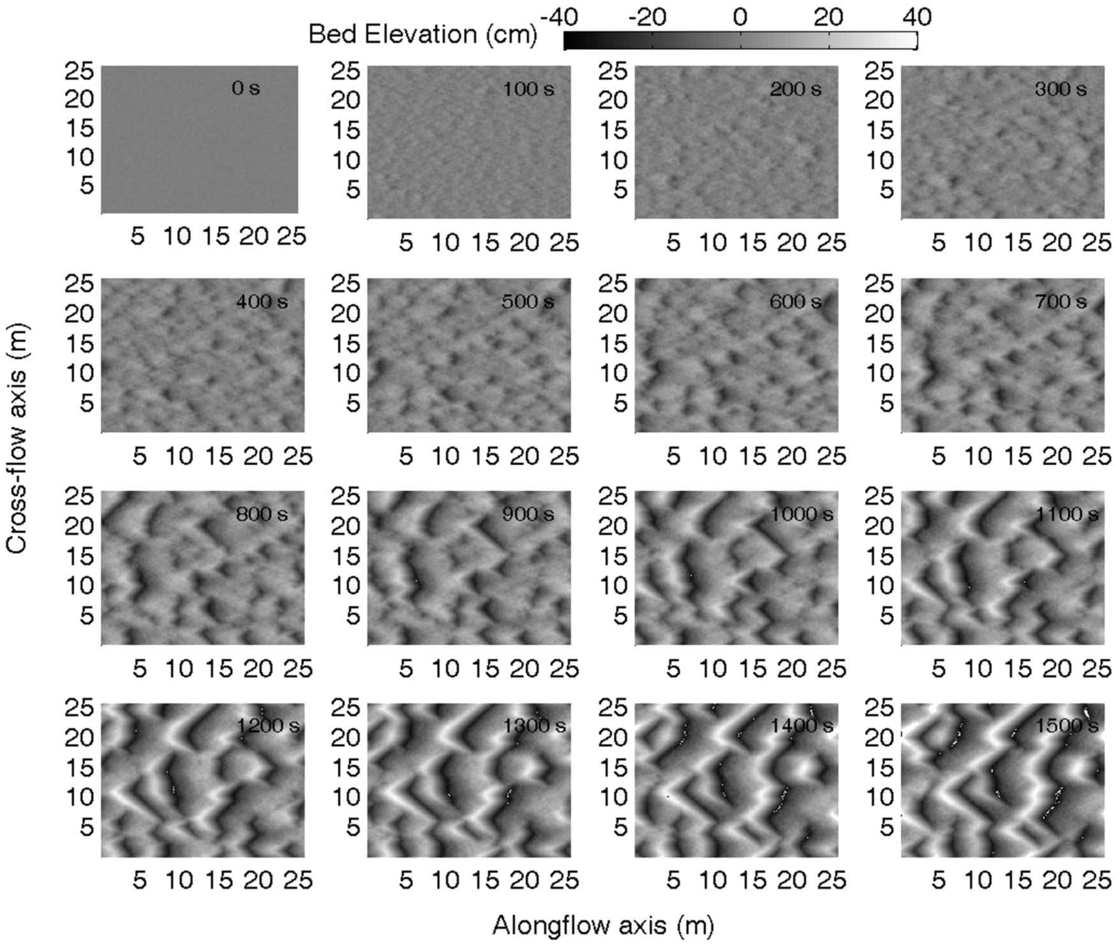

Figure 3. Bed form evolution. Using conditions identical to Figure 2a (transport via simple rules using a sinusoidal flow with A = 75 cm/s, S = 20 cm/s, T = 10 s, va = 15 cm/s) bed form evolution is shown at 100 s intervals and continues to 1500 s.

sport rates are higher, bed forms grow more quickly and if transport rates are lower, bed forms grow more slowly. However, as long as sediment is moved with the flow and the feedback mechanisms are in place, realistic bed forms will develop, thus supporting the hierarchical approach and the concept of self-organization.

[24] Regime-type models and most empirical models for predicting the height and length of bed forms assume that there is an equilibrium condition that is reached and that bed forms will stop growing when that condition is satisfied [e.g., *Wiberg and Harris*, 1994; *Nielsen*, 1981; *Clifton*, 1976]. Thus, these models predict a single bed form height and length for a given flow condition. Observations from the natural surf zone by CW04 indicated that megaripples grew continuously unless they were destroyed (when conditions changed too quickly, or in the extremely shallow water of the swash, or under breaking waves at the seaward edge of the surf zone). They found that the lengths of megaripples less than 12 h old grew quickly and linearly and beyond 12 h, growth slowed and became logarithmic. Here predicted megaripple lengths are also observed to grow, quickly at first and then their growth slows. Logarithmic curves (straight lines on the semilog plot, found by minimizing the mean square error between the curve and the model data, Figure 5) represent the early growth of modeled bed forms better than the linear relationship observed by CW04 (shown as curved lines in Figure 5). However, despite the different functional representations used for the CW04 field data and the model data, the two data sets are still comparable. Both grow quickly at first and then transition rather abruptly to slower growth.

[25] The transition times from early fast growth to later slower growth are used as a measure of growth rate. When using sinusoidal fluid forcing (e.g., Figure 2b), the model transition time (~25 min or 1500 s) is much shorter than the natural time scale of 12 h (Figure 5, red dots). To simulate a more natural growth rate, cross-shore velocities from the natural surf zone (the shore-perpendicular component only) measured with an electromagnetic current meter in about 2 m water depth (about 0.5 m above the seafloor) were used to drive the model instead of the sinusoidal flow. A data record was chosen from a period when megaripples were known to exist [*Gallagher et al.*, 1998] and the predicted bed after 4.2 h (~15,000 s) using measured flows to force the *Ribberink* [1998] transport formulation is shown in Figure 2h. When run with the real velocity record, the growth of the modeled bed forms is slower, with the transition at ~50 min (Figure 5, blue dots). However, this is still much faster than the natural bed form growth with the

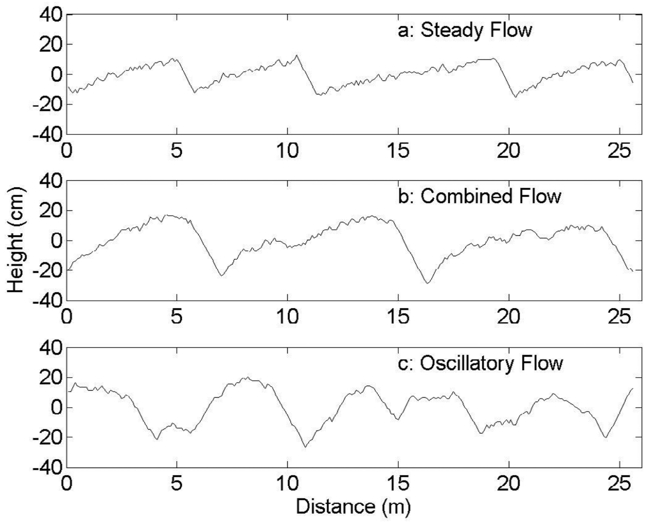

Figure 4. Profiles across simulated bed forms along lines marked in Figures 2a, 2f, and 2g.

transition at 12 h. (Note that CW04 estimated megaripple wavelength directly from images, whereas, in this study, wavelength is estimated from bed spectra. This could cause some discrepancy in comparisons of wavelengths and their growth but does not explain the unrealistically fast formation times in the model.)

[26] The difference in growth rate of modeled versus natural megaripples may be explained by examining the velocity records. The largest amplitudes of the natural cross-shore velocity from the measured time series are over 100 cm/s and the root mean square (RMS) is 32 cm/s. The modeled sinusoidal flows have amplitudes of 75 cm/s and a RMS of 65 cm/s. This difference is because the measured velocities are skewed (with the strongest flows having a short duration) and irregular, with the largest velocities (>75 cm/s) occurring infrequently. So under natural flows, high transport rates are intermittent. In contrast, the sinusoidal flows reach their maximum velocity every cycle and drive high rates of sand transport consistently. Therefore, bed forms are built more quickly under the consistent sinusoidal flows and more slowly under the variable natural flows. Neither flow field reproduces the natural growth rate and transition time of 12 h observed by CW04. The long transition time observed in

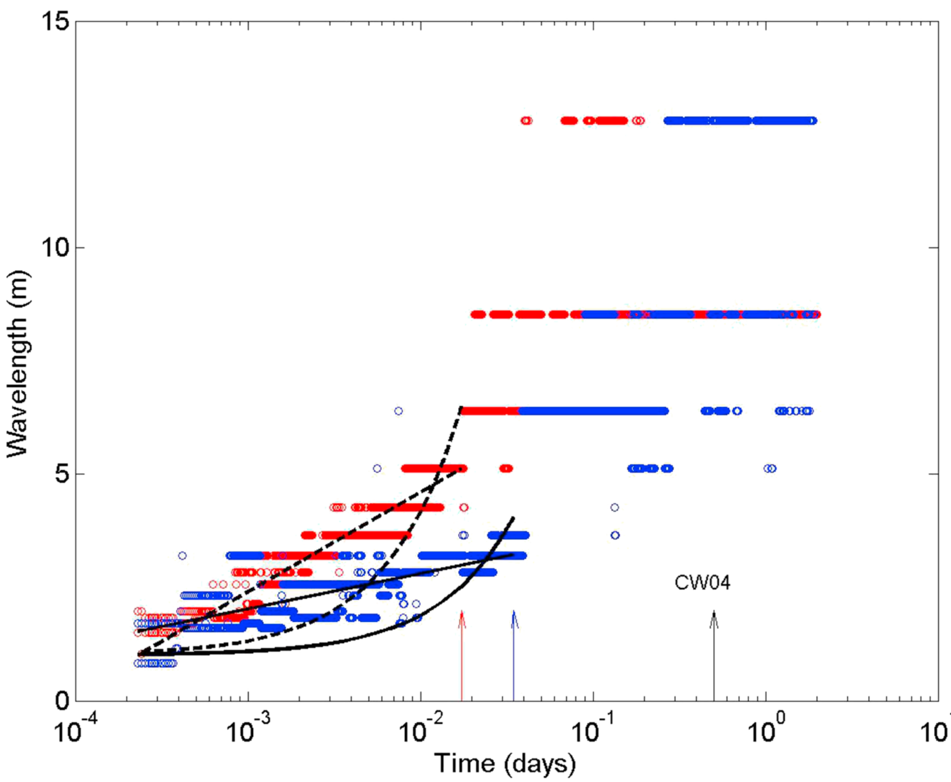

Figure 5. Modeled megaripple wavelength plotted versus time driven by sinusoidal flows (red dots) and natural flows (blue dot), both using the *Ribberink* [1998] transport formulation. Lines represent the log (straight lines) and linear (curved lines) fits to the modeled data for sinusoidal flows (dashed lines) and natural flows (solid lines). Arrows show the transition time estimated from the log fit to the early fast growth for the different model data sets (arrow colors match dots). The black arrow shows the transition time from the natural data of CW04. To estimate wavelength, spectra were calculated using an $n = 256$ point FFT for each along-flow (x) line in the model domain (e.g., Figure 2), all of which were averaged to give a single spectrum for each bed time point. The inverse of the wave number at the peak of the spectrum is used for wavelength.

the natural surf zone likely results from the even higher variability of the total flow field, including more realistic turbulence, more realistic acceleration on the bed form crest (acting to reduce amplitude growth), variation in direction (here only one-dimensional, shore-perpendicular flows are considered), variation in tidal level, which CW04 state is the dominant controller of the magnitude of the depth-dependent, wave-driven flows in the surf zone [*Raubenheimer*, 2002], and possibly the frequent interruption of the feedback mechanisms (see discussion below) by turbulence from breaking waves. In addition, some morphology modeling studies include diffusion terms to slow high growth rates and smooth excessively large bed forms [e.g., *Marieu et al.*, 2008]. No diffusion mechanism is used here, but one may be explored in future model studies. However, with both flows tested here (sinusoidal and measured), similar bed forms are built with similar dynamics, suggesting that the model captures the basic bed form generation mechanisms correctly.

[27] *Werner and Kocurek* [1999] attributed the change from early fast growth to later slower growth to a dynamical transition. Early in bed form growth, mergers between short-crested bed forms with many defects (crest terminations) are observed. As the short-crested features become longer-crested features, there are fewer defects and the defects are observed to migrate through the bed form field. Bed forms continue to grow through the migration of defects through the bed form field, but this process is much slower than the initial merging of many short-crested bed forms. Thus, as the number of defects decreases, the growth rate slows and the bed forms mature.

[28] To compare the present model to the *Werner and Kocurek* [1999] model for bed form dynamics, the number of defects was estimated manually from snapshots of the modeled bed forms (e.g., Figure 3). In this case, defects were identified, not as crest terminations, but as trough terminations, because the troughs are more visible and identifiable than crests. The number of defects is large at the start of the model runs (Figure 6) because there are many small irregular, short-crested bumps or proto-bed forms (these are difficult to identify). However, the number of defects decreases quickly as the short-crested proto-bed forms merge creating more discrete bed forms. After recognizable megaripples begin to dominate, the number of defects decreases, quickly at first then more slowly as the bed forms merge. At this point, the migration of defects through the bed form field, as described by *Werner and Kocurek* [1999], is observed in the present model. Note that the transition times in Figure 6 (denoted by arrows at ~1500 s or ~25 min for sinusoidal flow and at ~3000 s or ~50 min for the real surf zone flow) correspond well with the times when wavelength growth rate changes in Figure 5. Thus, the increase in wavelength through merging of smaller bed forms and the reduction of defects, described by *Werner and Kocurek* [1999], explains well the dynamics observed in the present model. Here both wavelength growth and defect density reduction continue until they are constrained by domain size. A more quantitative comparison with *Werner and Kocurek* [1999] was not possible because crest length (which is an independent variable in their work) is difficult to establish with these modeled bed forms. In addition, the present bed forms are crescentic which violates assumptions in the *Werner and Kocurek* [1999] model and perhaps explains the functional difference in Figure 5 (between the log fit and the linear fit). However, these results qualitatively are in excellent agreement with *Werner and Kocurek* [1999].

[29] The presence of more irregular flows (as in the natural surf zone) likely acts to maintain defects and slow bed form growth. For example, directionally varying nearshore flows (oscillatory flows, cross-shore flows like rips, alongshore currents, and their temporal variabilities) work to alter the directionality of the bed form field. In an earlier paper, *Werner and Kocurek* [1997] discussed how bed forms were turned in directionally varying flows via bed form motion at the defects (or the ends of the bed form crests). CW04 observed that bed forms would be wiped out if the flow direction changed too quickly for the bed form field to adjust. Thus, it is likely that a directionally varying flow could create a balance between growth processes (defect migration and mergers) and destruction processes, where defects are maintained or created for altering bed form directionality. This type of balance would result in significantly slower bed form growth than is predicted here (or perhaps even complete destruction). Similarly, highly turbulent flows, like those in the nearshore, add to the irregularity both in direction, magnitude, and frequency, which could maintain defects and slow bed form growth. Another mechanism that could further reduce bed form growth in the nearshore is the interruption of the shadow-zone feedback mechanism (Figure 1a), which acts to build bed forms. If this mechanism is interrupted by strong vertical velocities owing to breaking waves, the growth of the bed forms will be slowed (more below). So it is hypothesized that the highly variable natural flows in the nearshore will alter and slow the growth of bed forms.

[30] CW04 observed the destruction of bed forms in the swash and breaker zones. The changes in the velocity field in these regions are complicated and their physics are not explicitly modeled here. In the swash, the feedback relationship between the bed and the flow is altered owing to the extremely shallow water. In other words, as the bed forms become depth-limited (whether through growth or falling tide), the flow over the crest of the bed form accelerates (owing to flow constriction), transport increases at the crest, and the slopes of the bed form are reduced. With a reduced slope, the shadow zone is diminished. Therefore, the smoothing, crest acceleration feedback mechanism is strengthened and the bed form building, shadow zone mechanism is reduced. Similarly, excessive turbulence under breaking waves can be injected into the bottom boundary layer [*Fedderson et al.*, 2003] and the feedback relationship between the flow and the bed can be interrupted. Here these phenomena are modeled simply by removing the velocity shadow feedback mechanism (Figure 1a). Beginning with the established bed forms in Figure 2a, removing the velocity shadow feedback mechanism and allowing the bed to evolve for another 13 min results in almost complete destruction of bed forms (Figure 2i). This result supports the depth-based predictive model of CW04 and suggests that as long as the given flow bed feedback relationship is intact the associated bed forms will continue to evolve. When that relationship is interrupted (in the shallow swash or under breaking waves), bed forms and their growth will be altered, slowed, or destroyed.

[31] In the natural surf zone, long-crested megaripples sometimes are observed [*Gallagher*, 2003], but more often

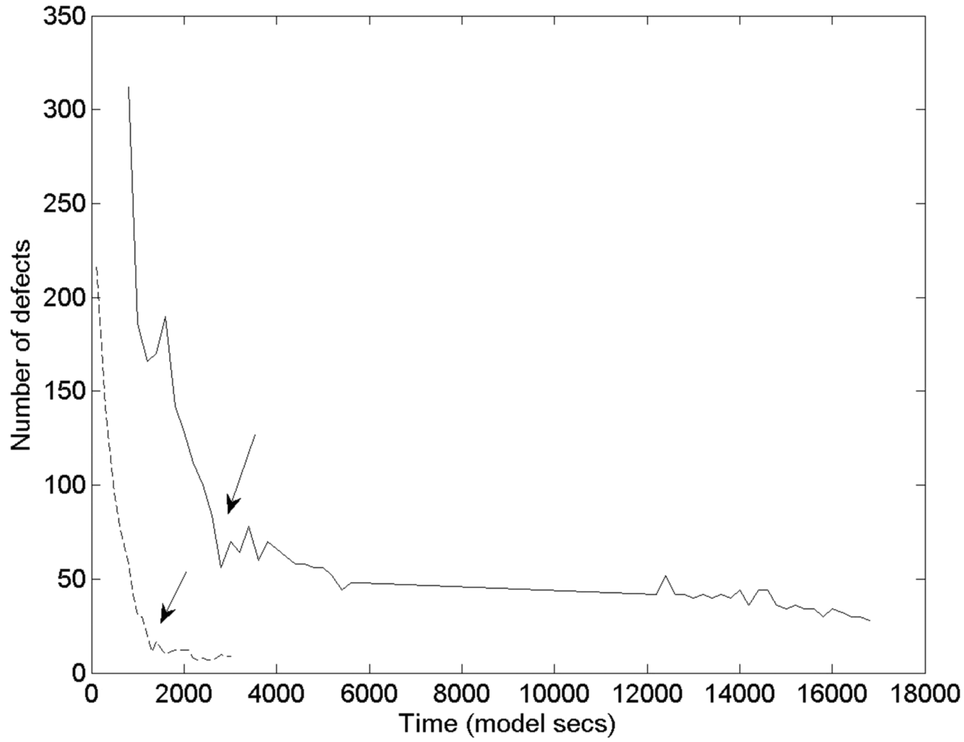

Figure 6. The number of defects (trough terminations) plotted versus time in elapsed model seconds. Defects were counted manually from images of the modeled bed form domain every 100 (or 200) s (e.g., Figure 3). Defects were identified as the end of each visible bed form trough. The solid line represents defect density versus time for the model run using the measured surf zone velocities (as in Figure 2h). The dashed line represents defect density versus time for the sinusoidal flow field (with conditions identical to Figure 3). The arrows identify roughly the location where the defects density decrease slows down.

megaripples are shorter-crested, three-dimensional, lunate, or oval-shaped features [*Gallagher et al.*, 1998; *Ngusaru and Hay*, 2004; *Hay and Wilson*, 1994]. *Gallagher* [2003] observed relatively long-crested megaripples just outside the surf zone and while the more three-dimensional features occurred inside the surf zone. The present model results suggest that this observation may be attributable to breaking wave-induced turbulence and directionally and temporally variable waves and wave-driven currents within the surf zone, causing an increase in defect creation and maintenance and a reduction in the growth rate of bed forms or regular destruction and reformation of bed forms (CW04). Thus, the highly changeable flow field in the surf zone results in relatively young, three-dimensional bed forms on average. In contrast, the more consistent (shore-normal waves giving a smooth oscillatory flow without breaking-induced turbulence or currents) flow field just outside the breaking waves allows bed forms to lengthen and mature.

5. Conclusion

[32] A self-organization model successfully predicts megaripples in the combined flows of the nearshore. The modeled creation, development, and destruction of these realistic bed forms support the concepts of hierarchical modeling, self-organization, and emergent behavior. The dynamics of modeled bed forms suggests that an initial perturbation is necessary to generate irregularities on the bed and that feedback mechanisms, which respond to those irregularities, are extremely important for bed form growth and continued development. The model reproduces the fast and then slow growth observed in the natural surf zone by CW04 (although the model growth rate is much faster than the natural megaripples). Thus, the present model behaves as predicted by *Werner and Kocurek* [1999], with defect density being an important dynamic variable in predicting wavelength growth rate. This dynamic growth pattern suggests that bed forms in the natural surf zone are not, in general, in equilibrium with the flow field and that they grow, migrate, and change continuously. Eventual equilibrium of nearshore megaripples may be possible, but the highly variable environment of the surf zone (with turbulence, breaking, depth changes owing to tides, offshore wave variability, and temporally variable currents) may preclude the possibility of equilibrium.

Appendix A: Model Sensitivity

[33] There are a number of variables and parameters in the transport models for which published values were used (Table 2). Most of these values will affect the outcome of the model in that they change the magnitude of the transport. By increasing calculated transport values, bed forms form and grow more quickly and under reduced transport con-

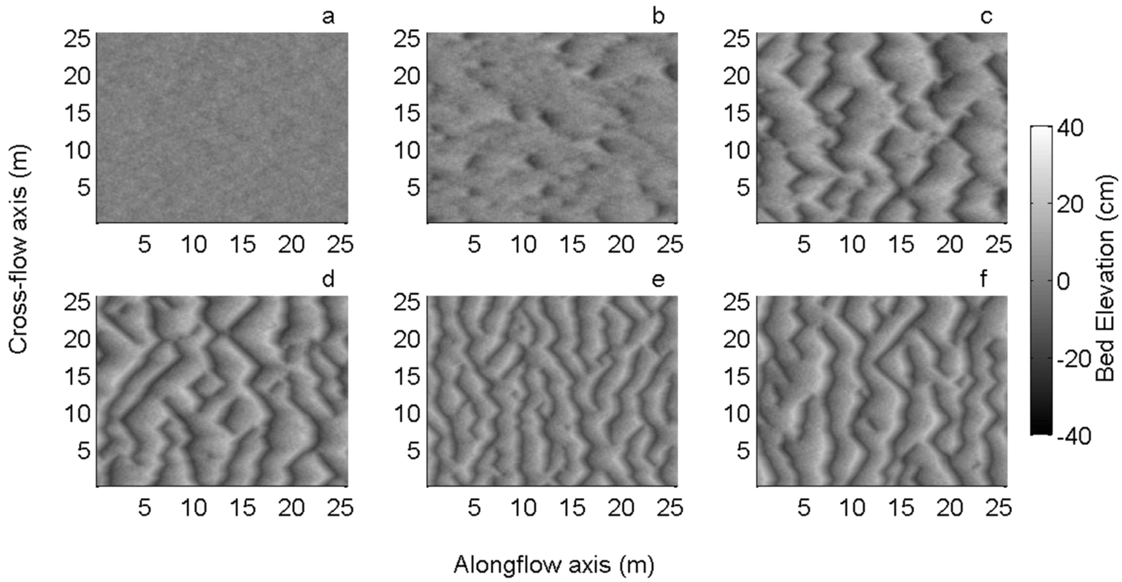

Figure A1. Examples of predicted bed forms using conditions the same as in Figure 2b, except that the jump fraction *jf* has been varied with (a) *jf* = 0.1, (b) *jf* = 0.067, (c) *jf* = 0.05, (d) *jf* = 0.04, (e) *jf* = 0.025, and (f) *jf* = 0.025, but the model has now been run for an additional 13 min.

ditions they grow more slowly. Bed forms will not form if the calculated transport magnitude is never large enough to pick up blocks, that is when $Q < \sim 1$ cm^3/s which occurs for $u \sim 70$ cm/s using *Ribberink* [1998] or $u \sim 70$ cm/s for the simple rules formulation (derived from *Bailard* [1981]). For this study, values from the literature were chosen for the well-known model parameters (C_f, ε_b, ε_s, f_w; see Table 2), and sensitivity to these was not tested further.

[34] The sensitivity to grain size (D in the *Ribberink* [1998] formulation and W in the *Bailard* [1981] formulation) was tested qualitatively. Because grain size is not explicitly accounted for in the modeled sediment bed, changing grain size changes only the magnitude of the transport calculated from the equations, which changes the number of sand blocks picked up. If grain size is set higher, fewer slabs are picked up and the speed with which bed forms form and grow is reduced. For example, bed forms predicted with a fall velocity $W = 1.5$ cm/s (corresponding to a grain size of about 100–200 μm) are shown in Figure 2a. (Figure 2a uses the simple rules transport formulation with thresholds estimated from *Bailard* [1981] using $W = 1.5$ cm/s). If W is increased to 3 cm/s for sediments ~300 μm, transport rate is effectively reduced, less sand is picked up for a given water velocity, and the bed forms take longer to grow. If W is increased further to 9 cm/s (for ~600 μm sand), bed forms no longer form and grow. This is because, using the same velocity field (with $A = 75$ cm/s and $S = 20$ cm/s), the flow is almost never large enough to exceed the transport threshold to pick up one block (Table 1).

[35] The sensitively to model parameters discussed above refers to parameters in the transport formulations and therefore changes in the magnitude of calculated transport used to pick up blocks of sand. Once sediment blocks are lifted from the bed using the transport formulations, they are moved using the water velocity and the jump fraction *jf* (equation (4)). Possible values of *jf* range from 0.1 to about 0.01. As mentioned earlier, if *jf* is larger than 0.1, sediment will move further than the water particles, which is physically unrealistic. For *jf* close to 0.1, sediments move long distances with each jump as sediments suspended in the flow would. Here when *jf* is high, bed forms either do not form or are highly irregular and three-dimensional (Figures A1a and A1b). This is interpreted as being the result of sand bypassing the feedback mechanism as might happen in strong sheet flow that suppresses bed form formation and smoothes the bed. High *jf* values could also be interpreted as representing fine grain sizes. In this case, grains will be subject to high suspended load transport rates and will travel long distances before settling to the bed (again bypassing the feedback mechanism). For small *jf* ~ 0.01, only the highest velocities ($u > 100$ cm/s) will be able to move sand forward, which is accurate for very large grain sizes. Clearly, *jf* is a model parameter that is dependent on the grain size. Here we are looking at beach sands, and *jf* was taken to be 0.05, an intermediate value with which the sediment moves about half the distance of the free stream water particles.

[36] The dependence on *jf* is illustrated in Figure A1, using conditions identical to Figure 2b. In Figure A1a, with *jf* = 0.1, no bed forms were created (and no bed forms were created when the model was allowed to run twice as long). In Figure A1b, with *jf* = 0.067, bed forms are created, but they are irregular and three-dimensional (and stay that way for longer model runs). In Figures A1c–A1e, with *jf* = 0.05, 0.04, and 0.025, similar bed forms are created but for smaller *jf*, they are less developed with shorter wavelengths. In Figure A1f, the case in Figure A1e with *jf* = 0.025 was allowed to run for an additional 13 min and those bed forms continued to lengthen and mature, finally looking similar to the bed forms in Figure A1d. Thus, as with changes in transport magnitude, changes in jump distance have the effect of speeding, slowing, or impeding the growth of bed

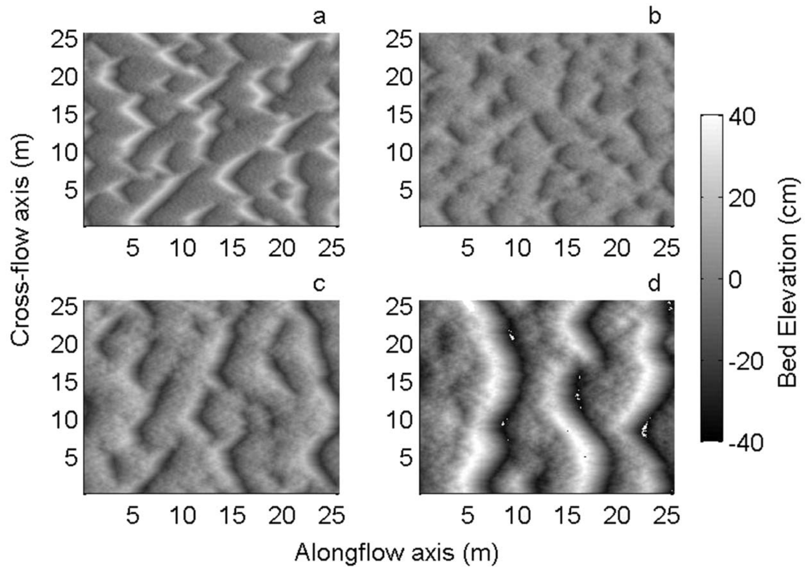

Figure A2. Examples of predicted bed forms using conditions the same as in Figure 2b, except that the turbulence amplitude *va* has been varied with (a) *va* = ±5 cm/s, (b) *va* = ±15 cm/s (same as Figure 2b), (c) *va* = ±50 cm/s, and (d) *va* = ±100 cm/s.

forms. For *jf* values above about 0.7 bed forms will not grow easily owing to long jump distances and the bypassing of feedback mechanisms. Below that threshold, smaller *jf* values translate to lower transport and slower growth.

[37] The "turbulence," as implemented in the model, does affect growth rate and bed form morphology (Figure A2). The turbulence is implemented (e.g., in Figures 2 and 3) as a spatially random velocity variation with amplitude *va* = ±15 cm/s added to the velocity field at each grid square (10 cm × 10 cm) and at each time point (1 s). Thus, it is random in space and it changes for each time point in the model run. When turbulence amplitude *va* is increased, the largest transport magnitudes in the domain are higher and therefore bed form growth rates are faster (compare Figures A2b, A2c, and A2d). (Because transport is nonlinearly related to velocity, larger velocities generate much larger transport magnitudes, while lower velocities still produce little to no transport.) However, increased *va* also results in an increased variation in the spatial distribution of velocities, which affects the spatial bed form patterns making bed forms smoother and less distinct (compare Figures A2a and A2b). As implemented, the turbulence is rather artificial with only one spatial scale (10 cm × 10 cm) and one time scale (1 s). At this time, improvements on this simplistic model component are being tested.

[38] **Acknowledgments.** This study was supported by a grant from the National Science Foundation, ADVANCE Fellows Program (0340758), and a grant from the Office of Naval Research–Coastal Geosciences (N00014-10-1-0643). I would like to thank Giovanni Coco for great advice and collegiality throughout this project. Three anonymous reviews and one by Brad Werner were extremely useful in improving this paper.

References

Ahl, V., and T. F. H. Allen (1996), *Hierarchy Theory*, Columbia Univ. Press, New York.

Austin, M. J., G. Masselink, T. J. O'Hare, and P. E. Russell (2007), Relaxation time effects of wave ripples in tidal beaches, *Geophys. Res. Lett.*, *34*, L16606, doi:10.1029/2007GL030696.

Bagnold, R. A. (1941), *The Physics of Blown Sand and Desert Dunes*, 265 pp., Methuen and Co. Ltd., London.

Bagnold, R. A. (1966), An approach to the sediment transport problem from general physics, *U.S. Geol. Surv. Prof. Pap.*, *422-I*, 37 pp.

Bailard, J. A. (1981), An energetics total load sediment transport model for a plane sloping beach, *J. Geophys. Res.*, *86*(C11), 10,938–10,954, doi:10.1029/JC086iC11p10938.

Blondeaux, P. (2001), Mechanics of coastal forms, *Annu. Rev. Fluid Mech.*, *33*, 339–370.

Church, J. C., and E. B. Thornton (1993), Effects of breaking wave induced turbulence within a longshore current model, *Coastal Eng.*, *20*, 1–28.

Clarke, L. B., and B. T. Werner (2004), Tidally modulated occurrences of megaripples in a saturated surf zone, *J. Geophys. Res.*, *109*, C01012, doi:10.1029/2003JC001934.

Clifton, H. E. (1976), Wave-formed sedimentary structures-A conceptual model, in *Beach and Nearshore Sedimentation*, *Spec. Publ.*, *24*, edited by R. A. Davis and R. L. Ethington, pp. 126–148, SEPM, Tulsa, Okla.

Clifton, H. E., R. E. Hunter, and R. L. Phillips (1971), Depositional structures and processes in the non-barred high-energy nearshore, *J. Sediment. Petrol.*, *41*(3), 651–670.

Coco, G., and A. B. Murray (2007), Patterns in the sand: From forcing templates to self-organization, *Geomorphology*, *91*, 271–290.

Coco, G., D. A. Huntley, and T. J. O'Hare (2000), Investigation of a self-organization model for beach cusp formation and development, *J. Geophys. Res.*, *105*(C9), 21,991–22,002, doi:10.1029/2000JC900095.

Duke, W. L., R. W. C. Arnott, and R. J. Cheel (1991), Shelf sand stones and hummocky cross-stratification; New insights on a stormy debate, *Geology*, *19*(6), 625–628.

Dyer, K. R., and D. A. Huntley (1999), The origin, classification and modeling of sand banks and ridges, *Cont. Shelf Res.*, *19*(10), 1285–1330.

Ernstsen, V. B., R. Noormets, C. Winter, D. Hebbein, A. Bartholoma, B. W. Fleming, and J. Bartholdy (2005), Development of subaqueous barchanoid-shaped dunes due to lateral grain size variability in a tidal inlet channel of the Danish Wadden Sea, *J. Geophys. Res.*, *110*, F04S08, doi:10.1029/2004JF000180.

Fedderson, F., E. L. Gallagher, R. T. Guza, and S. Elgar (2003), The drag coefficient, bottom roughness, and wave-breaking in the nearshore, *Coastal Eng.*, *48*, 189–195.

Fredsoe, J., and R. Deigaard (1992), Mechanics of coastal sediment transport, in *Advance Series on Coastal Engineering*, vol. 3, World Sci., London.

Gallagher, E. L. (2003), A note on megaripples in the surf zone: Evidence for their relation to steady flow dunes, *Mar. Geol.*, *193*, 171–176.

Gallagher, E. L., S. Elgar, and E. B. Thornton (1998), Megaripple migration in a natural surf zone, *Nature*, *394*, 165–168.

Gallagher, E. L., E. B. Thornton, and T. P. Stanton (2003), Sand bed roughness in the nearshore, *J. Geophys. Res.*, *108*(C2), 3039, doi:10.1029/2001JC001081.

Gallagher, E. L., S. Elgar, R. T. Guza, and E. B. Thornton (2005), Estimating nearshore bed form amplitudes with altimeter, *Mar. Geol.*, *216*, 51–57.

Garcez-Faria, A. F., E. B. Thornton, T. P. Stanton, C. M. Soares, and T. C. Lippmann (1998), Vertical profiles of longshore currents and related bed shear stress and bottom roughness, *J. Geophys. Res.*, *103*(C2), 3217–3232, doi:10.1029/97JC02265.

Hay, A. E., and T. Mudge (2005), Principal bed states during SandyDuck97: Occurrence, spectral anisotropy and the bed state storm cycle, *J. Geophys. Res.*, *110*, C03013, doi:10.1029/2004JC002451.

Hay, A. E., and R. Speller (2005), Naturally occurring scour pits in nearshore sands, *J. Geophys. Res.*, *110*, F02004, doi:10.1029/2004JF000199.

Hay, A. E., and D. J. Wilson (1994), Rotary side scan images of nearshore bed form evolution during a storm, *Mar. Geol.*, *119*, 57–65.

Hulscher, S. J. M. H. (1996), Tidal-induced large-scale regular bed form patterns in a three-dimensional shallow water model, *J. Geophys. Res.*, *101*(C9), 20,727–20,744, doi:10.1029/96JC01662.

Idier, D., D. Astruc, and S. J. M. H. Hulscher (2004), Influence of bed roughness on dune and megaripple generation, *Geophys. Res. Lett.*, *31*, L13214, doi:10.1029/2004GL019969.

Jerolmack, D. J., and D. Mohrig (2005), A unified model for subaqueous bed form dynamics, *Water Resour. Res.*, *41*, W12421, doi:10.1029/2005WR004329.

Kessler, M. A., and B. T. Werner (2003), Self-organization of sorted patterned ground, *Science*, *299*, 380–383.

Marieu, V., P. Bonneton, D. L. Foster, and F. Ardhuin (2008), Modeling of vortex ripple morphodynamics, *J. Geophys. Res.*, *113*, C09007, doi:10.1029/2007JC004659.

Meyer-Peter, E., and R. Mueller (1948), Formulas for bed load transport, paper presented at 2nd International Association for Hydraulic Research Congress, Stockholm, Sweden.

Middleton, G. V., and J. B. Southard (1984), *Mechanics of Sediment Transport, Short Course 3*, 401 pp., Soc. for Econ. Paleontol. and Mineral., Tulsa, Okla.

Ngusaru, A. S., and A. E. Hay (2004), Cross-shore migration of lunate megaripples during Duck94, *J. Geophys. Res.*, *109*, C02006, doi:10.1029/2002JC001532.

Nielsen, P. (1981), Dynamics and geometry of wave-generated ripples, *J. Geophys. Res.*, *86*(C7), 6467–6472, doi:10.1029/JC086iC07p06467.

Nishimori, H., and N. Ouchi (1993), Formation of ripple patterns and dunes by wind-blown sand, *Phys. Rev. Lett.*, *71*, 197–200.

Nittrouer, J. A., M. A. Allison, and R. Campanella (2008), Bed form transport rates for the lowermost Mississippi River, *J. Geophys. Res.*, *113*, F03004, doi:10.1029/2007JF000795.

Raubenheimer, B. (2002), Observations and predictions of fluid velocities in the surf and swash zones, *J. Geophys. Res.*, *107*(C11), 3190, doi:10.1029/2001JC001264.

Raudkivi, A. J. (1990), *Loose Boundary Hydraulics*, 538 pp., Pergamon, New York.

Ribberink, J. S. (1998), Bed-load transport for steady flows and unsteady oscillatory flows, *Coastal Eng.*, *34*, 59–82.

Sterlini, F., S. J. M. H. Hulscher, and D. M. Hanes (2009), Simulating and understanding sand wave variation: A case study of the Golden Gate sand waves, *J. Geophys. Res.*, *114*, F02007, doi:10.1029/2008JF000999.

Stolum, H. (1996), River meandering as a self-organization process, *Science*, *271*, 1710–1713.

Thornton, E. B., R. T. Humiston, and W. Birkemeier (1996), Bar/trough generation on a natural beach, *J. Geophys. Res.*, *101*(C5), 12,097–12,110, doi:10.1029/96JC00209.

Werner, B. T. (1995), Eolian dunes: Computer simulations and attractor interpretation, *Geology*, *23*, 1107–1110.

Werner, B. T. (1999), Complexity in natural landform patterns, *Science*, *284*, 102–104.

Werner, B. T., and G. Kocurek (1997), Bed-form dynamics: Does the tail wag the dog?, *Geology*, *25*, 771–774, doi:10.1130/0091-7613(1997)025<0771:BFDDTT>2.3.CO;2.

Werner, B. T., and G. Kocurek (1999), Bed form spacing from defect dynamics, *Geology*, *27*, 727–730.

Wiberg, P. L., and C. K. Harris (1994), Ripple geometry in wave-dominated environments, *J. Geophys. Res.*, *99*(C1), 775–790, doi:10.1029/93JC02726.

E. L. Gallagher, Department of Biology, Franklin and Marshall College, PO Box 3003, Lancaster, PA 17604, USA. (edith.gallagher@fandm.edu)